Mark S. Humayun
James D. Weiland
Gerald Chader
Elias Greenbaum (Eds.)

# Artificial Sight

## Basic Research, Biomedical Engineering, and Clinical Advances

Springer

Mark S. Humayun
James D. Weiland
Gerald Chader
Doheny Eye Institute
Los Angeles, CA 90033
USA
humayun@doheny.org
jweiland@doheny.org
gchader@doheny.org

Elias Greenbaum
Oak Ridge National Laboratory
Oak Ridge, TN 37831
USA
greenbaum@ornl.gov

ISBN-13: 978-0-387-49329-9 e-ISBN-13: 978-0-387-49331-2

Library of Congress Control Number: 2006939422

© 2007 Springer Science+Business Media, LLC.
All rights reserved. This work may not be translated or copied in whole or in part without the written permission of the publisher (Springer Science+Business Media, LLC., 233 Spring Street, New York, NY 10013, USA), except for brief excerpts in connection with reviews or scholarly analysis. Use in connection with any form of information storage and retrieval, electronic adaptation, computer software, or by similar or dissimilar methodology now known or hereafter developed is forbidden.
The use in this publication of trade names, trademarks, service marks and similar terms, even if they are not identified as such, is not to be taken as an expression of opinion as to whether or not they are subject to proprietary rights.

Printed on acid-free paper.

9 8 7 6 5 4 3 2 1

springer.com

# 18
# Electrical Stimulation of Mammalian Retinal Ganglion Cells Using Dense Arrays of Small-Diameter Electrodes

Chris Sekirnjak[1], Pawel Hottowy[2], Alexander Sher[3], Wladyslaw Dabrowski[2], Alan M. Litke[3] and E. J. Chichilnisky[1]

[1]*The Salk Institute for Biological Studies*
[2]*Faculty of Physics and Applied Computer Science, AGH University of Science and Technology*
[3]*Santa Cruz Institute for Particle Physics, University of California*

**Abstract:** Current epiretinal implants contain a small number of electrodes with diameters of a few hundred microns. Smaller electrodes are desirable to increase the spatial resolution of artificial sight. To lay the foundation for the next generation of retinal prostheses, we assessed the stimulation efficacy of micro-fabricated arrays of 61 platinum disk electrodes with diameters 8–12 μm, spaced 60 μm apart. Isolated pieces of rat, guinea pig, and monkey retina were placed on the multi-electrode array ganglion cell side down and stimulated through individual electrodes with biphasic, charge-balanced current pulses. Spike responses from retinal ganglion cells were recorded either from the same or a neighboring electrode. Most pulses evoked only 1–2 spikes with short latencies (0.3–10 ms), and rarely was more than one recorded ganglion cell stimulated. Threshold charge densities for eliciting spikes in ganglion cells were typically below 0.15 mC/cm$^2$ for pulse durations between 50 and 200 μs, corresponding to charge thresholds of ~ 100 pC. Stimulation remained effective after several hours and at frequencies up to 100 Hz. Application of cadmium chloride did not abolish evoked spikes, implying direct activation. Thus, electrical stimulation of mammalian retina with small-diameter electrodes is achievable, providing high temporal and spatial precision with low charge densities.

## Introduction

Electrical stimulation of retinas in blind people has demonstrated the potential for direct excitation of retinal neurons as a means of re-establishing sight [1]. The retina in patients with advanced neurodegenerative diseases

(such as retinitis pigmentosa or age-related macular degeneration) contains very few photoreceptors, but a substantial fraction of ganglion cells remain intact [2, 3]. Epiretinal implants specifically target surviving ganglion cells by positioning stimulating electrodes in close proximity to the inner surface of the retina.

In spite of recent successes, the present-day implants are but a small step toward restoring meaningful sight. Psychophysical studies indicate that foveal implants which create useful vision must contain a minimum of about 600 electrodes [4]. To achieve this number or greater, electrodes must be tightly packed, necessitating small stimulation sites. At present, the resolution is exceedingly crude and the density of electrodes per implant area is low: a typical epiretinal implant contains a few electrodes with diameters of several hundred microns, spaced hundreds of microns apart [1].

Useful artificial vision will require implants with hundreds or thousands of much smaller electrodes. Ideally, an advanced implant would devote one electrode to every ganglion cell and each electrode would be similar in size to the cell it is designed to stimulate (tens of microns). Little is known about the parameters which would permit reliable retinal stimulation with electrodes which approach cellular dimensions. When the electrode surface area is reduced, current and charge densities increase drastically, and high charge densities are known to cause tissue damage by electrochemical reactions [5–7].

A review of the pertinent literature reveals that the feasibility of stimulation with arrays of small electrodes in mammalian tissue has not been adequately tested. The majority of studies involving retinal stimulation have used needle-shaped probes such as platinum wires or concentric microelectrodes [8–10]. Others have attempted to utilize smaller stimulating microprobes with tip diameters of 25 $\mu$m or less [11–14]. The geometry of such probes differs greatly from the planar disk electrode design developed for current epiretinal implants. Stimulation is always limited to a single stimulation site, prohibiting the study of stimulation using multiple electrodes, their interactions, and crosstalk effects. The use of multi-electrode arrays for retinal stimulation has been mainly limited to large electrodes with diameters between 100 and 1500 $\mu$m [15–18]. While multi-electrode arrays with smaller electrodes have been utilized to selectively stimulate the axons of retinal ganglion cells [19, 20] and to stimulate the retina in the subretinal space [21, 22], no study has reported the use of electrodes with surface areas below 200 $\mu m^2$ to target mammalian ganglion cells.

The goal of this study was to establish current and charge thresholds for stimulation of rat, guinea pig, and primate retina using small electrodes with surface areas of 50–100 $\mu m^2$ (corresponding to diameters of 8–12 $\mu$m). In this manner, this study directly addresses the prevalent concerns about the usability of small electrodes for retinal prosthetics. Our two-dimensional multi-electrode arrays use planar disk microelectrodes very similar to those utilized in present epiretinal prosthetics, but smaller by 1–2 orders of magnitude.

# Materials and Methods

## *Retinal Preparation*

This study utilized retinal tissue from 17 adult rats, 4 guinea pigs, and one macaque monkey. The average body weight was $284 \pm 7$ g for rats, $386 \pm 52$ g for guinea pigs, and 4 kg for the macaque monkey.

Rodent eyes were enucleated after decapitation of animals deeply anesthetized with 10 mg/kg Xylazine and 50 mg/kg Ketamine HCl. Primate eyes were obtained from terminally anesthetized macaque monkeys (Macaca radiata) used by other experimenters. Immediately after enucleation, the anterior portion of the eye and vitreous were removed in room light and the eye cup placed in bicarbonate-buffered Ames' solution.

Pieces of retina 1–2 mm in diameter (Figure 18.1) were separated from the retinal pigment epithelium and placed flat on the electrode array, with the ganglion cell layer facing the array. The tissue was held in place by weighted nylon netting positioned gently over the array. The preparation was then mounted on a circuit board attached to an inverted microscope and continuously superfused at room temperature with Ames' solution bubbled with 95% oxygen and 5% carbon dioxide. Enucleation, vitrectomy, and dissections were performed in normal laboratory lighting conditions, likely resulting in substantial retinal photobleaching.

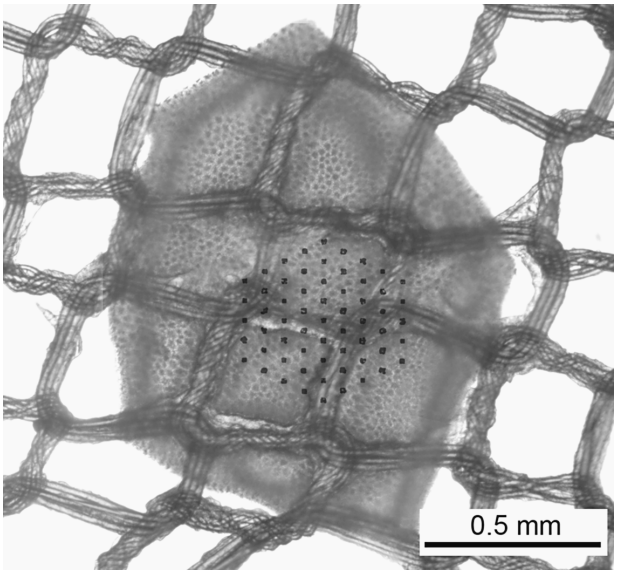


FIGURE 18.1. A retinal tissue piece on the stimulation/recording setup, photographed during an experiment. The hexagonal multi-electrode array is visible in the center. The nylon netting applies gentle pressure on the tissue.

In several experiments (10 cells), cadmium chloride (100–250 μM) was added directly to the perfusion solution to block synaptic transmission. An increase in spontaneous bursting activity was observed, confirming that the drug efficiently diffused into the ganglion cell layer.

## *Multi-Electrode Array*

The array consisted of a planar hexagonal arrangement of 61 extracellular electrodes, approximately $0.5 \times 0.5\,\text{mm}^2$ in total size (Figure 18.2). These electrodes were used both to record action potentials extracellularly from ganglion cells [23, 24] and to apply current to the tissue for stimulation. The array was microfabricated on a glass substrate, with indium tin oxide leads and a silicone nitride insulation layer [25, 26]. Each electrode was formed by microwells (holes in the insulation layer) which were filled (electroplated) with platinum prior to an experiment. A platinum wire integrated into the array chamber served as indifferent ground, several millimeters away. All stimulations were performed using a monopolar configuration (electrode to distant ground).

## *Stimulation and Recording*

Experiments were performed on a setup allowing for simultaneous recording of all 61 electrodes and stimulation on multiple electrodes. The array was connected to a circuit board containing two microchips which multiplexed the 61 signals

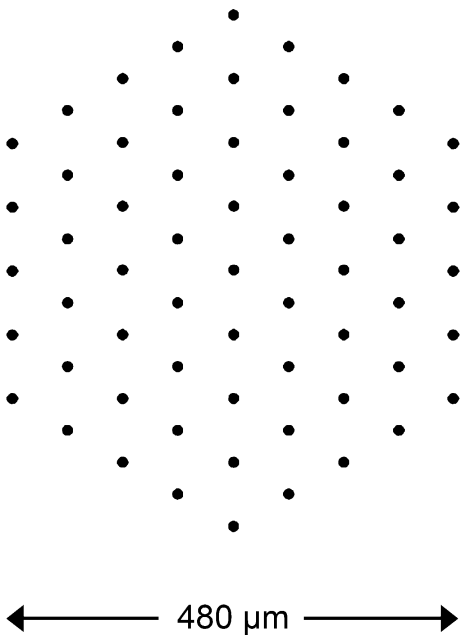


FIGURE 18.2. The hexagonal multi-electrode array. Electrode diameter varied between approximately 8 and 12 μm, with a fixed inter-electrode spacing of 60 μm.

and sent them to digitizing cards installed in a PC [25]. A dim level of illumination was maintained during the entire experiment (room lights or microscope illuminator). Recording and stimulation were controlled by interface software, and extracellular potentials were recorded from all 61 electrodes, digitized at 20 kHz [27], and stored for off-line analysis on a PC.

The stimulus pulse consisted of a negative square-wave current pulse of amplitude $A$ and duration $d$, followed immediately by a positive pulse of amplitude $A/2$ and duration $2d$. Reported current values always refer to the negative phase amplitude $A$; pulse duration always refers to the duration $d$ of the negative phase. All pulses were individually calibrated to produce biphasic stimuli with zero net charge. Stimulation frequency was varied between 0.25 and 100 Hz.

Many ganglion cells fire spontaneous spikes in isolated pieces of retina. Stimulation on a particular electrode was usually attempted only if spontaneous extracellular spikes could be recorded from that electrode. This approach guaranteed that the electrode was properly platinized and confirmed that ganglion cells in its vicinity were capable of firing action potentials. Typically, about half of the platinized electrodes on an array showed spontaneous activity from at least one cell.

Stimulation was attempted by using the lowest current settings and was then increased systematically if no response was seen. Threshold was defined as the current setting which produced a spike with nearly every stimulus pulse (approximately 95% of trials) during stimulation at 1–2 Hz.

Multi-electrode data were analyzed offline using Labview 6, Matlab 6, and Igor Pro 5. Means and group data were calculated in Microsoft Excel. Errors reported are standard errors of the mean (SEM), unless otherwise stated. Images were processed in Adobe Photoshop 7.

## *Digital Artifact Subtraction*

To reveal spikes with latencies of less than 1 ms, we developed an artifact subtraction method, which takes advantage of the fact that near threshold some stimulation trials will result in evoked spikes and some will fail to evoke responses. Short-latency spikes obscured by the stimulation artifact (which typically lasted for several milliseconds) were made visible by increasing the stimulation current until a possible spike threshold was reached. Just below threshold, the recorded traces changed shape noticeably on about half of the stimulus trials (for example, a change in curvature or peak height), indicating that a possible spike was elicited. Traces containing such possible spikes were averaged and subtracted from the average over those traces without spikes. Subtracting the failures from the successful stimulations eliminated the artifact and cleanly revealed the recorded ganglion cell spike. In general, this method was successful only in recordings with exceptionally short stimulation artifacts.

# Results

## *Evoked Spikes and Thresholds*

Our objective was to elicit spikes in ganglion cells by passing current through electrodes on the multi-electrode array. Stimulation at individual electrodes with currents up to 3 μA resulted in evoked spikes recorded at latencies between a few hundred μs and tens of ms. Of the 64 successfully stimulated ganglion cells, 45 were from rat, 11 from guinea pig, and 8 from monkey.

The majority of successful stimulation attempts yielded a single spike that often resembled the spontaneous spikes recorded at that particular electrode. In such experiments, the same electrode was used to stimulate and to record the response. Figure 18.3 shows three examples of spikes evoked in monkey, guinea pig, and rat retina, respectively. The average threshold current for 11 rat cells stimulated under identical conditions with 0.1 ms pulses was $0.66 \pm 0.03\,\mu A$, corresponding to a charge of 66 pC and a charge density of $0.08\,mC/cm^2$. In all three species, typical charge densities at threshold were consistently below $0.35\,mC/cm^2$, an often-stated safe limit for stimulation with platinum electrodes [28]. Stimulation using low amplitudes such as these usually affected only cells in the immediate vicinity of the stimulation electrode: of 86 analyzed neighboring electrodes in 17 stimulation experiments, only two were an evoked spikes from a different cell observed. However, evoked spikes from different cells were frequently seen on neighboring electrodes when the current was increased several-fold, indicating current spread to locations about 60 μm (the inter-electrode spacing) from the stimulation site.

## *Short-Latency Spikes*

To reveal the earliest spike responses following stimulation onset, the stimulus artifact was digitally subtracted from recorded traces (see Section "Digital artifact subtraction"). Figure 18.4 shows an example of a short-latency response obscured by the artifact. Averaging and artifact subtraction revealed a spike at sub-millisecond latency which resembled the spontaneous spike recorded at the same electrode (inset). Of 13 subtracted short-latency spikes (latency $0.77 \pm 0.15$ ms; range 0.2–1.9 ms), 12 closely matched the spontaneous spikes observed on the same electrode.

## *Threshold-Duration Curves*

Spike threshold was defined as the current amplitude which produced spikes at approximately 95% of trials and depended strongly on stimulus pulse duration. To quantify the relationship between threshold and duration, pulses with a range of durations between 50 μs and 1 ms were used for stimulation. Figure 18.5 shows that in all three species, higher currents were required to evoke a spike when shorter pulses were used. No systematic species difference was observed.

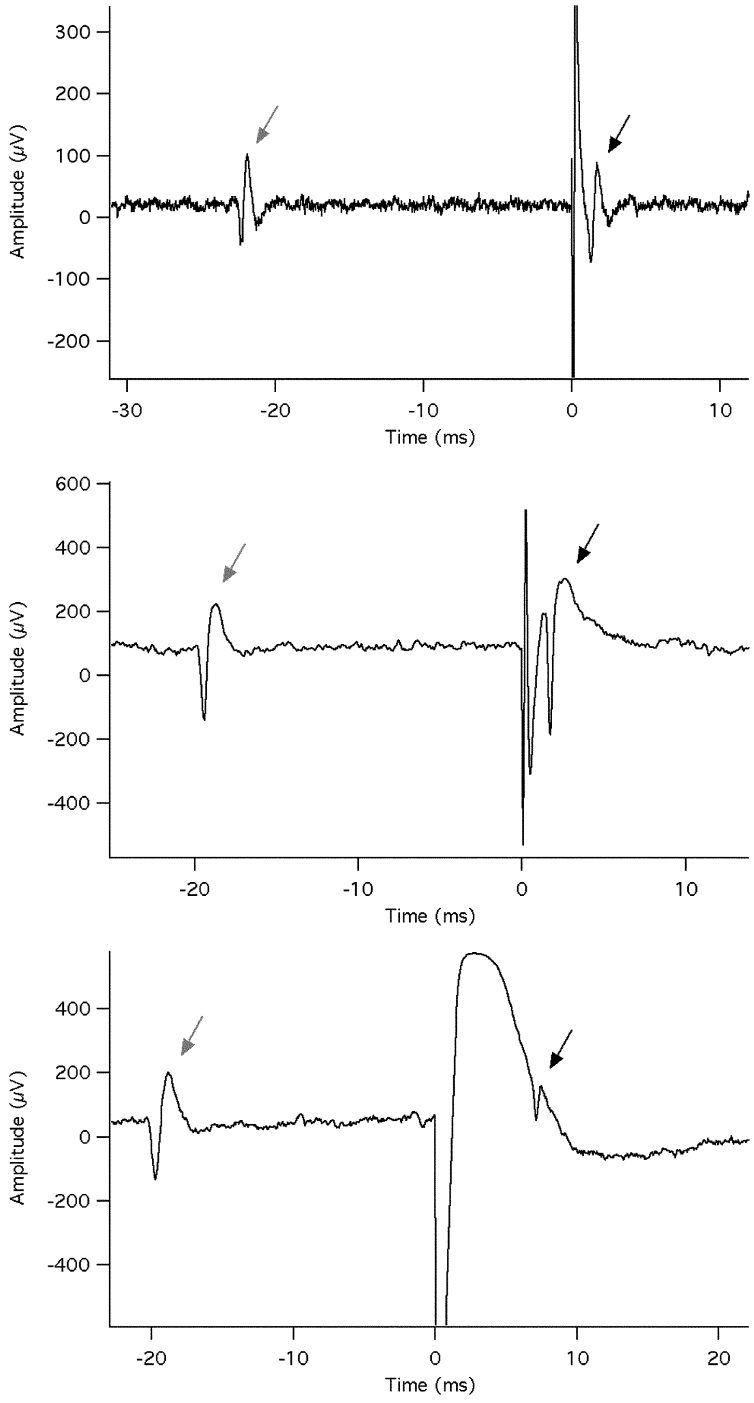


FIGURE 18.3. Examples of spikes evoked by electrical stimulation in three mammalian species. Top: monkey retina; middle: guinea pig retina; bottom: rat retina. Each example includes a spontaneous spike (gray arrow), a stimulus artifact (at time 0 ms), and a single evoked spike (black arrow). In the top two examples, the evoked spike is identical in shape to the spontaneous spike, while in the bottom trace it is distinct, indicating that a different cell was stimulated.

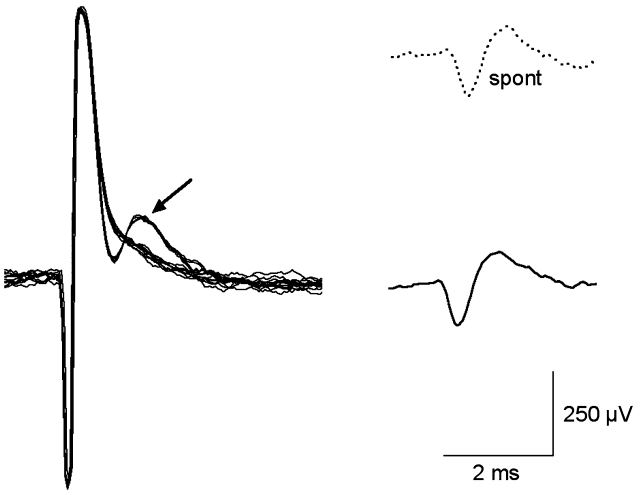


FIGURE 18.4. Artifact subtraction (rat retina). Left: overlay of 10 stimulation trials, some of which evoked a spike (arrow). Right: digitally subtracted spike with latency 0.55 ms. Top right: a spontaneous spike recorded from the same cell.

Exponential functions were fit to the data in Figure 18.5 by least-square regression and the resulting best-fit curves were used to estimate chronaxie (defined as the lowest stimulus duration required to elicit a response when using twice the minimum threshold amplitude). The average value for 12 cells was $196 \pm 66\,\mu s$.

## *Simultaneous Stimulation*

Functional artifical vision will likely require stimulation with many closely spaced electrodes. We tested the feasibility of spatial stimulation patterns by utilizing the multi-electrode array to stimulate at several electrodes at the same time. Figure 18.6 shows an example of simultaneous multi-site stimulation: spikes were evoked in two different ganglion cells by stimulating at two different electrodes with $0.6\,\mu A$ pulses. Each electrode was first stimulated on its own to establish thresholds and latencies. The two evoked responses had similar but not identical threshold currents and different latencies (5 and 9 ms). Stimulation at one electrode did not evoke spikes at the neighboring site, indicating that the responses could be elicited independently of each other. Evoking independent spikes on multiple electrodes spaced $60\,\mu m$ apart is thus feasible.

## *High Frequencies and Long Stimulation*

Ganglion cells are capable of firing at frequencies of up to 100–200 Hz in response to visual stimuli [29]. High-frequency electrical stimulation is a requirement for retinal prosthetics, since sustained percepts of light must be

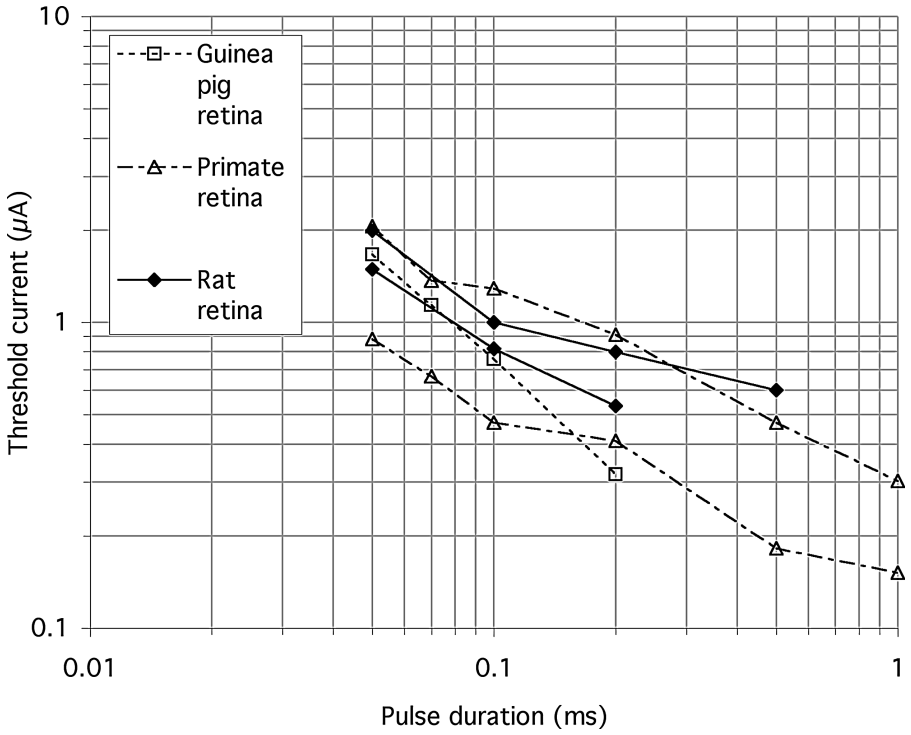


FIGURE 18.5. Threshold–duration relationships. Current necessary to evoke a spike is plotted as a function of pulse duration for 5 cells from three species.

generated. We used our setup to successfully stimulate 3 cells at frequencies up to 100 Hz. At such frequencies, spikes evoked at longer latencies (>2 ms) showed a dramatic decrease in response rate, while short-latency spikes could be evoked much more reliably.

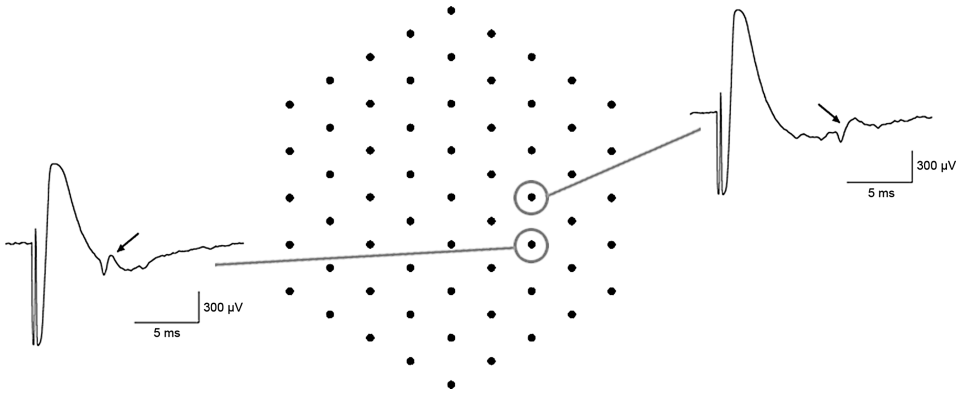


FIGURE 18.6. Simultaneous stimulation at multiple sites. Two nearby electrodes on the array were used to stimulate two ganglion cells independently of each other. The spike responses (arrows) are shown on the left and right, respectively.

Furthermore, human chronic retinal implants must be capable of delivering effective stimulation pulses over a period of many hours each day. To demonstrate that electrical stimulation remained functional after longer periods of time, two ganglion cells were stimulated continuously at 1–2 Hz for the longest duration that was experimentally feasible in our setup: spikes could still be evoked reliably after 4.5 hours, albeit with small threshold increases.

### *Miscellaneous Results*

To ascertain that the applied electrical pulses directly stimulated ganglion cells, the calcium channel blocker cadmium chloride (100–250 μM) was applied to the bath solution to abolish synaptic transmission. In all 10 cells tested, evoked spikes were still observed after drug application, indicating that the observed spikes were not produced by mechanisms involving calcium-dependent synaptic transmission.

To establish upper limits for electrical stimulation using our multi-electrode arrays, several cells were stimulated with very high charge densities. Stimulation at currents and charge densities several-fold above threshold tended to disrupt the spontaneous and evoked spikes of ganglion cells, usually in a reversible manner: spike height decreased until spikes could no longer be detected. In many cells, spiking activity resumed after a period of several minutes. Local toxicity or heating effects were likely responsible for disrupting ganglion cell spiking, indicating that there is an upper ceiling for the optimal range of currents used in stimulation using small array electrodes.

## Discussion

Electrical stimulation of rat, guinea pig, and primate retina with dense, small-diameter electrode arrays was achieved using low charge densities. Our multi-electrode arrays closely resemble those currently in use for human patient testing but contain much smaller electrodes at a much smaller electrode spacing. The purpose of this study was to elucidate the basic stimulation parameters so that the next generation of implants may incorporate a design using much smaller electrodes than are currently in use.

An important concern regarding implantable stimulation devices is their capability to deliver electrical current that is safe, yet efficient. As shown in this study, a single ganglion cell (at most a few cells) can be induced to fire a single spike (at most a few spikes) by using currents typically below 1 μA and with charge densities below 0.10 $mC/cm^2$. The literature is inconclusive about the safety of small electrodes for prosthetic implants: reported threshold values range from 0.16 $mC/cm^2$ [13] to 0.59 $mC/cm^2$ [14] for small-diameter microprobes, whereas 0.35 $mC/cm^2$ is the safe limit for stimulation with platinum electrodes [28]. We conclude that small-diameter electrode arrays (8–12 μm) do not require dangerously high charge densities to achieve reliable spiking in mammalian retina.

To determine the effectiveness of small-diameter electrodes, it would be of interest to record the neuronal activity in the vicinity of the stimulation electrode. However, stimulation and recording through the same small electrode brings about technical challenges. A large stimulus artifact obscures early spikes and others have reported that this artifact renders recording the response to stimulation near ganglion cell somas unfeasible [20]. While such technical limitations biased most of our observations to longer latency spikes ($>1$ ms), artifact subtraction performed on a few stimulated cells clearly revealed an early response at latencies of a few hundred $\mu$s. We speculate that most long latency stimulations also evoked an obscured short latency spike. Furthermore, since high-frequency stimulation tended to abolish long-latency spikes, we assume that the shortest-latency spikes will be the most significant during actual stimulation of human retina.

Small electrodes such as those used here typically only record spikes from cells located a short distance from the electrode. The shape of most evoked spikes resembled the spontaneous spike recorded at the recording electrode, indicating that the same nearby ganglion cell was stimulated. Taken together with the results of our neighbor-analysis, we conclude that currents around 1 $\mu$A usually do not activate cells outside a $\sim$30 $\mu$m radius around the stimulating electrode.

The simultaneous stimulation experiment provided evidence for the feasibility of simultaneous stimulation with a fixed current pulse amplitude at multiple sites, such as would be necessary in a retinal prosthesis. It further demonstrates that two neighboring electrodes can stimulate two cells independently and without crosstalk. While only two electrodes were used here, an epiretinal implant would utilize hundreds or thousands of stimulation sites to achieve artificial sight. Our findings suggest that stimulation with high spatial resolution is feasible using small electrodes.

In summary, safe and effective stimulation of mammalian retina with small planar electrodes is clearly feasible with high temporal and spatial precision. Future generations of epiretinal prosthetics should aim toward a design incorporating electrodes whose size approaches cellular dimensions.

*Acknowledgments.* This research was supported by the Salk Institute Pioneer Postdoctoral Fellowship, Second Sight Medical Products Inc., McKnight Foundation NEI grant 13150 (EJC), NEI grant 12893 (SSMP), NSF Awards PHY-0245104 and PHY-0417175 (AML), Polish State Committee for Scientific Research, Project 3 T11E 011 27 (WD), and NATO Collaborative Linkage Grant (AML & WD).

## *References*

1. Humayun M (2003) Clinical trial results with a 16-electrode epiretinal implant in end-stage RP patients. In: The First DOE International Symposium on Artificial Sight. Fort Lauderdale, FL: Department of Energy.
2. Santos A, Humayun MS, de Juan E, Jr., Greenburg RJ, Marsh MJ, Klock IB, Milam AH (1997) Preservation of the inner retina in retinitis pigmentosa. A morphometric analysis. Arch Ophthalmol 115:511–515.

3. Humayun MS, Prince M, de Juan E, Jr., Barron Y, Moskowitz M, Klock IB, Milam AH (1999) Morphometric analysis of the extramacular retina from postmortem eyes with retinitis pigmentosa. Invest Ophthalmol Vis Sci 40:143–148.
4. Cha K, Horch KW, Normann RA (1992) Mobility performance with a pixelized vision system. Vision Res 32:1367–1372.
5. Pollen DA (1977) Responses of single neurons to electrical stimulation of the surface of the visual cortex. Brain Behav Evol 14:67–86.
6. Brummer SB, Robblee LS, Hambrecht FT (1983) Criteria for selecting electrodes for electrical stimulation: theoretical and practical considerations. Ann N Y Acad Sci 405:159–171.
7. Tehovnik EJ (1996) Electrical stimulation of neural tissue to evoke behavioral responses. J Neurosci Methods 65:1–17.
8. Humayun M, Propst R, de Juan E, Jr., McCormick K, Hickingbotham D (1994) Bipolar surface electrical stimulation of the vertebrate retina. Arch Ophthalmol 112:110–116.
9. Weiland JD, Humayun MS, Dagnelie G, de Juan E, Jr., Greenberg RJ, Iliff NT (1999) Understanding the origin of visual percepts elicited by electrical stimulation of the human retina. Graefes Arch Clin Exp Ophthalmol 237:1007–1013.
10. Suzuki S, Humayun MS, Weiland JD, Chen SJ, Margalit E, Piyathaisere DV, de Juan E, Jr. (2004) Comparison of electrical stimulation thresholds in normal and retinal degenerated mouse retina. Jpn J Ophthalmol 48:345–349.
11. Dawson WW, Radtke ND (1977) The electrical stimulation of the retina by indwelling electrodes. Invest Ophthalmol Vis Sci 16:249–252.
12. Wyatt J, Rizzo JF, Grumet A, Edell D, Jensen RJ (1994) Development of a silicon retinal implant: epiretinal stimulation of retinal ganglion cells in the rabbit. Invest Ophthalmol Vis Sci 35:1380. ARVO abstract.
13. Rizzo JF, Grumet AE, Edell D, Wyatt J, Jensen R (1997) Single-unit recording following extracellular stimulation of retinal ganglion cell axons in rabbits. Invest Ophthalmol Vis Sci 38:S40.
14. Jensen RJ, Rizzo JF, 3rd, Ziv OR, Grumet A, Wyatt J (2003) Thresholds for activation of rabbit retinal ganglion cells with an ultrafine, extracellular microelectrode. Invest Ophthalmol Vis Sci 44:3533–3543.
15. Hesse L, Schanze T, Wilms M, Eger M (2000) Implantation of retina stimulation electrodes and recording of electrical stimulation responses in the visual cortex of the cat. Graefes Arch Clin Exp Ophthalmol 238:840–845.
16. Walter P, Heimann K (2000) Evoked cortical potentials after electrical stimulation of the inner retina in rabbits. Graefes Arch Clin Exp Ophthalmol 238:315–318.
17. Humayun MS, Weiland JD, Fujii GY, Greenberg R, Williamson R, Little J, Mech B, Cimmarusti V, Van Boemel G, Dagnelie G, de Juan E (2003) Visual perception in a blind subject with a chronic microelectronic retinal prosthesis. Vision Res 43: 2573–2581.
18. Rizzo JF, 3rd, Wyatt J, Loewenstein J, Kelly S, Shire D (2003) Methods and perceptual thresholds for short-term electrical stimulation of human retina with microelectrode arrays. Invest Ophthalmol Vis Sci 44:5355–5361.
19. Grumet A (1999) Electric stimulation parameters for an epi-retinal prosthesis. In: Department of Electrical Engineering and Computer Science, p 144: Massachusetts Institute Of Technology.
20. Grumet AE, Wyatt JL, Jr., Rizzo JF, 3rd (2000) Multi-electrode stimulation and recording in the isolated retina. J Neurosci Methods 101:31–42.

21. Zrenner E, Stett A, Weiss S, Aramant RB, Guenther E, Kohler K, Miliczek KD, Seiler MJ, Haemmerle H (1999) Can subretinal microphotodiodes successfully replace degenerated photoreceptors? Vision Res 39:2555–2567.
22. Stett A, Barth W, Weiss S, Haemmerle H, Zrenner E (2000) Electrical multisite stimulation of the isolated chicken retina. Vision Res 40:1785–1795.
23. Meister M, Pine J, Baylor DA (1994) Multi-neuronal signals from the retina: acquisition and analysis. J Neurosci Methods 51:95–106.
24. Chichilnisky EJ, Baylor DA (1999) Receptive-field microstructure of blue-yellow ganglion cells in primate retina. Nat Neurosci 2:889–893.
25. Litke AM (1998) The retinal readout system: an application of microstrip detector technology to neurobiology. Nucl Instrum Methods Phys Res A 418:203–209.
26. Litke AM, Chichilnisky EJ, Dabrowskic W, Grilloa AA, Grybosc P, S. K, Rahmand M, G. T (2003) Large-scale imaging of retinal output activity. Nucl Instrum Methods Phys Res A 501:298–307.
27. Litke AM (1999) The retinal readout system: a status report. Nucl Instrum Methods Phys Res A 435:242–249.
28. Brummer SB, Turner MJ (1977) Electrical stimulation with Pt electrodes: II-estimation of maximum surface redox (theoretical non-gassing) limits. IEEE Trans Biomed Eng 24:440–443.
29. Wandell BA (1995) Foundations of Vision, Sunderland, MA: Sinauer.